

SINGULARITY AND MESH DIVERGENCE OF INVISCID ADJOINT SOLUTIONS AT SOLID WALLS

CARLOS LOZANO¹ AND JORGE PONSIN²

Computational Aerodynamics Group
National Institute of Aerospace Technology (INTA).
Carretera de Ajalvir, km 4. Torrejón de Ardoz 28850, Spain.
¹lozanorc@inta.es, ²ponsinj@inta.es

Key words: Adjoint Euler equations, Analytic adjoint solution, Wall singularity, Mesh Dependence.

Abstract. The mesh divergence problem occurring at subsonic and transonic speeds with the adjoint Euler equations is reviewed. By examining a recently derived analytic adjoint solution, it is shown that the explanation is that the adjoint solution is singular at the wall. The wall singularity is caused by the adjoint singularity at the trailing edge, but not in the way it was previously conjectured.

1 INTRODUCTION

Recently, it has been shown [1] [2] [3] [4] that in two and three dimensions, certain numerical adjoint solutions to the Euler equations have values at and near the surface of wings and airfoils that depend strongly on the mesh density and which do not converge as the mesh is refined. This phenomenon has been observed for lift-based adjoint solutions for any subcritical or transonic flow condition, including incompressible flow, while for drag-based adjoint solutions it has only been observed in transonic rotational flows.

The problem seems to be rather generic, as it has been found in solutions obtained with continuous and discrete adjoint schemes and with different solvers. Increasing the numerical dissipation with mesh refinement does not qualitatively change the behavior, although the actual value of the adjoint at the wall strongly depends on the level of numerical dissipation. It was conjectured in [1] that this behavior is likely caused by the adjoint singularity at the sharp trailing edge, although an understanding of the actual mechanism was lacking. It was subsequently pointed out that the anomaly is also correlated with the adjoint singularity along the incoming stagnation streamline predicted by Giles and Pierce [5], and it appears also in flows past blunt bodies without sharp trailing edges. Finally, recent evidence [6] involving linearized perturbations with point sources shows that there might actually be an adjoint singularity along the wall, with the same origin as the one along the incoming stagnation streamline. The presence of a singularity at the wall would certainly explain the behavior (it appears that, without dissipation, the adjoint values would grow unbounded), but it would

remain to determine if the singularity is of numerical or analytic origin and, in the latter case, how a singular (*i.e.* infinite) adjoint solution could be reconciled with the adjoint wall b.c.

The singularity along the incoming stagnation streamline for the adjoint Euler equations was predicted by using the exact solution for a Green's function involving perturbations to the stagnation pressure. This solution contains an integral along streamlines that appeared to be the source of the singularity along the incoming stagnation streamline, so it was an obvious point to start. Unfortunately, the analysis is based on a local examination of the integral around the leading stagnation point that does not directly apply to the present case. This motivated us to simplify the problem and try to work out the complete exact solution for incompressible (and irrotational) inviscid flow, for which at least two exact Green's functions (the point source and the point vortex) are known. This led to a complete closed form solution for the 2D adjoint incompressible Euler equations in [7], which we will use here to settle the issue once and for all.

2 REVIEW OF THE MESH DIVERGENCE PROBLEM

To introduce the problem, we examine a fairly simple example: the adjoint solution for inviscid incompressible flow at angle of attack $\alpha = 0^\circ$ past a symmetrical van de Vooren airfoil given by the conformal transformation [8]

$$z(\zeta) = \frac{(\zeta - R)^k}{(\zeta - \varepsilon R)^{k-1}} + 1 \quad (1)$$

where ε is a thickness parameter and k is related to the trailing-edge angle τ as $k = 2 - \tau / \pi$. The transformation maps the airfoil in the z plane to a circle of radius $R = (1 + \varepsilon)^{k-1} / 2^k$ centered at the origin in the ζ plane. In this paper, we set $\varepsilon = 0.0371$ and $k = 86/45$, resulting in an airfoil with 12% thickness and finite trailing edge angle $\tau = 16^\circ$ that closely resembles a NACA0012 airfoil (see Figure 1). This case is interesting because it has analytic solutions for both the flow [8] and lift and drag-based adjoint equations [7].

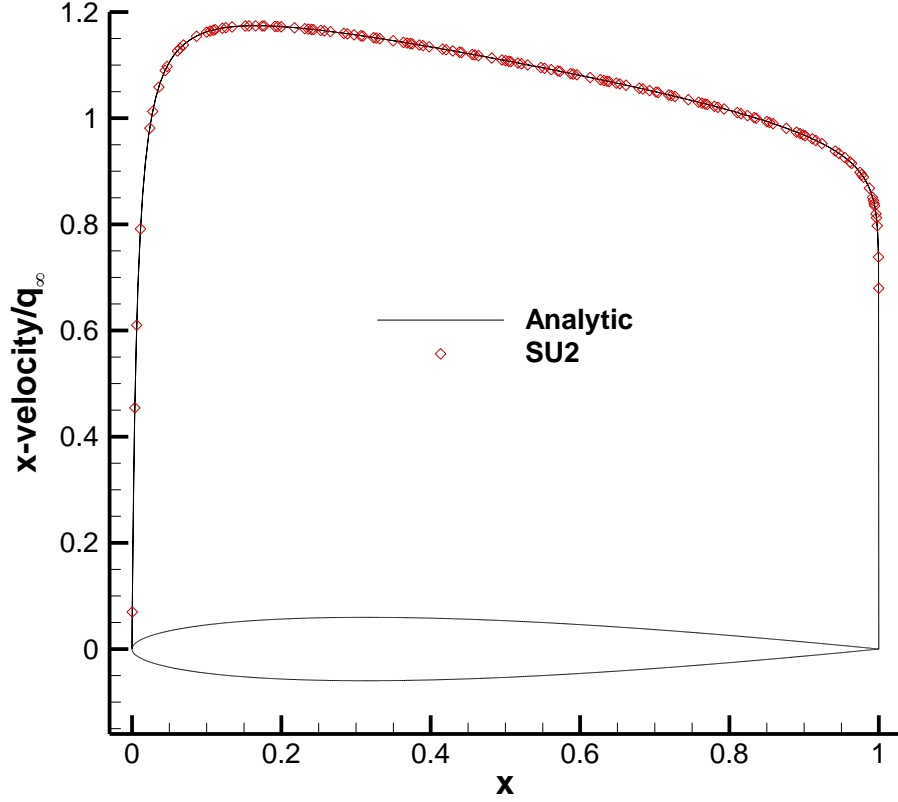


Figure 1. x -velocity for incompressible, inviscid flow past a van de Vooren airfoil with trailing-edge angle $\tau=16^\circ$ and 12% thickness computed with the SU2 solver and with conformal transformation techniques.

Given the above flow solution, we consider the lift or drag-based adjoint problem. For a more thorough introduction to the adjoint method, see for example [9]. The adjoint state $\psi^T = (\psi_1, \psi_x, \psi_y)$ obeys the adjoint Euler equation

$$\nabla \psi^T \cdot \vec{F}_U = 0$$

with adjoint wall boundary condition

$$(\psi_x, \psi_y) \cdot \vec{n}_s = \vec{d} \cdot \vec{n}_s$$

and far-field b.c.

$$\psi^T (\vec{F}_U \cdot \vec{n}_{s^\infty}) \delta U = 0.$$

Here $\vec{F}_U = \partial(\rho \vec{v}, \rho \vec{v}u + p\hat{x}, \rho \vec{v}v + p\hat{y})^T / \partial(p, \rho u, \rho v)$ is the (incompressible) flux Jacobian, p is the pressure, ρ is the (constant) density, $\vec{v} = (u, v)$ is the fluid velocity, $\delta U = (\delta p, \delta(\rho u), \delta(\rho v))^T$ is a linear flow perturbation, \vec{n}_s and \vec{n}_{s^∞} are outward pointing unit

normal vectors at the wall and far-field boundaries, respectively, and $\vec{d} = (\cos \alpha, \sin \alpha)$ for drag and $\vec{d} = (-\sin \alpha, \cos \alpha)$ for lift, respectively, where α is the angle of attack. This case should be straightforward to solve numerically, but turns out to yield unexpected results. Plotting the adjoint values on the airfoil profile across several mesh levels, one would expect to see at most a singularity at the trailing edge [10], with the solution along the remainder of the profile remaining stable or progressively converging over successive mesh levels. This is not what is observed, though. Figure 2 plots the drag and lift-based numerical adjoint solutions computed for the above case with the SU2 incompressible solver [11] on a sequence of progressively refined meshes. While the drag-based adjoint solution (left) behaves smoothly even at the trailing edge and converges with mesh refinement, the lift-based adjoint solution (right) diverges at the trailing edge on any given mesh, but also across the entire airfoil profile as the mesh density increases.

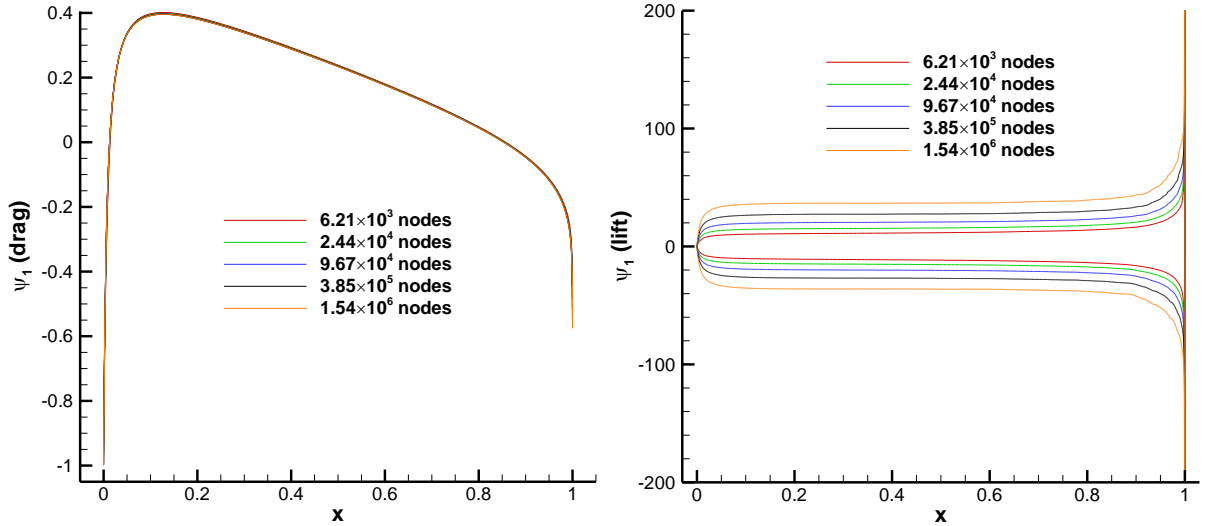


Figure 2. Drag (left) and lift (right)-based inviscid, incompressible adjoint solution on a van de Vooren airfoil at $\alpha = 0^\circ$ on 5 progressively refined unstructured triangular meshes computed with the SU2 solver.

This anomaly was originally found in [12] for the drag-based adjoint solution corresponding to two-dimensional, transonic inviscid flow past a NACA0012 airfoil at Mach number $M = 0.8$ and angle of attack $\alpha = 1.25^\circ$. In order to characterize the problem, the following tests were made in Refs. [1] [2] [3] [4]:

1. Viscous cases were investigated to determine if the anomaly is limited to inviscid cases. It is.
2. The effect of cost function and flow regime was tested, with the following results:

- For supersonic flow, lift or drag-based adjoint solutions do not show this behavior.
 - For transonic and subsonic flow, including incompressible flow, lift-based adjoint solutions are always affected, while drag-based solutions are only affected for transonic rotational flows (such as, for example, shocked flow past a symmetric airfoil with non-zero angle of attack).
 - The adjoint state based on the far-field entropy flux $\int_{S_\infty} s\vec{v} \cdot \hat{n} ds$, shows the same behavior as the near-field drag. This output function is not based on near-field computations and, accordingly, the adjoint wall boundary condition is simply $(\psi_x, \psi_y) \cdot \vec{n}_s = 0$ in this case [13].
3. Inviscid three dimensional cases were tested, yielding the same behavior.
 4. The behavior of the adjoint wall b.c. $(\psi_x, \psi_y) \cdot \vec{n}_s = \vec{d} \cdot \vec{n}_s$ with mesh refinement was investigated. It turned out to be reasonably well obeyed across mesh levels except in the immediate vicinity of the trailing edge.
 5. Given this anomalous behavior, it was mandatory to test whether adjoint-based sensitivity derivatives are affected. They are not. In fact, they are actually quite accurate and fairly stable across mesh levels.
 6. The problem was originally discovered with DLR's Tau code [14], which uses an unstructured, cell-vertex, finite-volume solver, and appeared in both the continuous and discrete adjoint solvers with upwind and central schemes with JST dissipation [15]. However, similar results have been obtained with the SU2 code, ONERA's structured, cell-centered ELSA code [6], and Imperial College's Nektar++ code [16].
 7. Originally, the anomaly was observed for an airfoil with nonzero trailing-edge angle. In order to determine the effect of the trailing edge geometry, several different configurations, including blunt and cusped trailing edges, were tested. The anomaly was observed in all cases, and also in blunt bodies (circles and ellipses).
 8. The effect of the far-field distance, resolution and the adjoint far-field b.c. was tested, but no significant influence could be established.
 9. The adjoint solutions were examined in order to establish whether the anomaly is related to any flow or adjoint singularity. It was found that the anomaly is always accompanied by the presence of an adjoint singularity at the trailing edge or rear stagnation point, but also along the incoming stagnation streamline. Conversely, when such singularities are absent, the adjoint solution converges with mesh refinement.
 10. The effect of numerical dissipation was tested by using a central scheme with JST artificial dissipation. On the one hand, mesh convergence studies were repeated with dissipation levels increasing with mesh size ($\varepsilon_2 \sim N^{1/2D}$, where ε_2 is the second

dissipation coefficient, N is the number of grid nodes and D is the number of spatial dimensions) without significant qualitative changes in the behavior. On the other hand, the actual value of the adjoint solution at the wall on a given mesh was shown to depend strongly on the dissipation level, in such a way that reducing the dissipation increases the value of the adjoint solution, mimicking the effect of mesh refinement.

11. In addition, it was shown in [6] (see also [4]) that the linear perturbation to the lift or drag caused by numerical solutions containing point singularities corresponding to stagnation pressure perturbations do appear to diverge towards the wall as the mesh is refined, while other point perturbations (mass, normal force or enthalpy, using the nomenclature of [5]) do not.

3 ANALYTIC ADJOINT SOLUTION FOR INCOMPRESSIBLE FLOW

So far, the explanation of the problem has been elusive. In [1], the anomaly was conjectured to be a numerical effect triggered by the adjoint singularity at the trailing edge, but no precise explanation of the actual mechanism responsible was given. Local mesh dependence near adjoint singularities is to be expected, but mesh dependence across the entire wall is puzzling unless one is willing to admit the presence of a singularity at the wall. This possibility was however ruled out in [1] based on the lack of positive evidence in the analysis carried out in [5] of the analytic properties of 2D adjoint solutions, which did not give any hint of an adjoint singularity at the wall but did not exclude it either.

Later on, the behavior of numerical solutions containing point singularities corresponding to stagnation pressure perturbations [6], whose effect on lift or drag can be computed via finite-differences with the non-linear solver or alternatively in terms of the corresponding adjoint state, started to hint at the existence of a singularity of the adjoint solution at the wall, the nature of which was however not completely elucidated. As discussed in [4], the presence of a singularity at the wall would certainly explain the behavior, but it would remain to determine if the singularity is of numerical or analytic origin and, in the latter case, how a singular (i.e. infinite) adjoint solution could be reconciled with the adjoint wall b.c.

With that in mind, the only possibility for further progress is to build an analytic solution using the Green's function approach [17], which however requires as many analytic Green's functions as there are equations (4 in 2D compressible flow, and 3 if the flow is incompressible). A promising candidate would be inviscid, incompressible flow past a two-dimensional airfoil. The flow is irrotational, so two exact Green's functions (the point source and the point vortex) are readily available. A third one is required, which can be taken to be a stagnation pressure perturbation as in [5], resulting in the closed-form analytic adjoint solutions for lift and drag obtained in [7]. The solutions are built in terms of a conformal mapping $z = F(\zeta)$ transforming an airfoil in the physical plane z into a circle of radius R and centered at $\zeta_0 = X_0 + iY_0$ in the

complex ζ -plane. The map transforms the point $\zeta_{te} = X_{te} + iY_{te}$ on the circle into the trailing edge of the airfoil at $z = 1$. The analytic solution for drag reads

$$\begin{pmatrix} \psi_1 \\ \psi_2 \\ \psi_3 \end{pmatrix}_{Drag} = \frac{1}{c_\infty q_\infty} \begin{pmatrix} q^2 - q_\infty^2 \\ q_\infty \cos \alpha - u \\ q_\infty \sin \alpha - v \end{pmatrix}$$

where $q^2 = u^2 + v^2$, which had been independently obtained in [18]. This is compared in Figure 3 with the SU2 numerical adjoint solution for the van der Vooren airfoil described earlier. The solution is smooth and analytic throughout, and lacks the singularities at the incoming stagnation streamline and trailing edge.

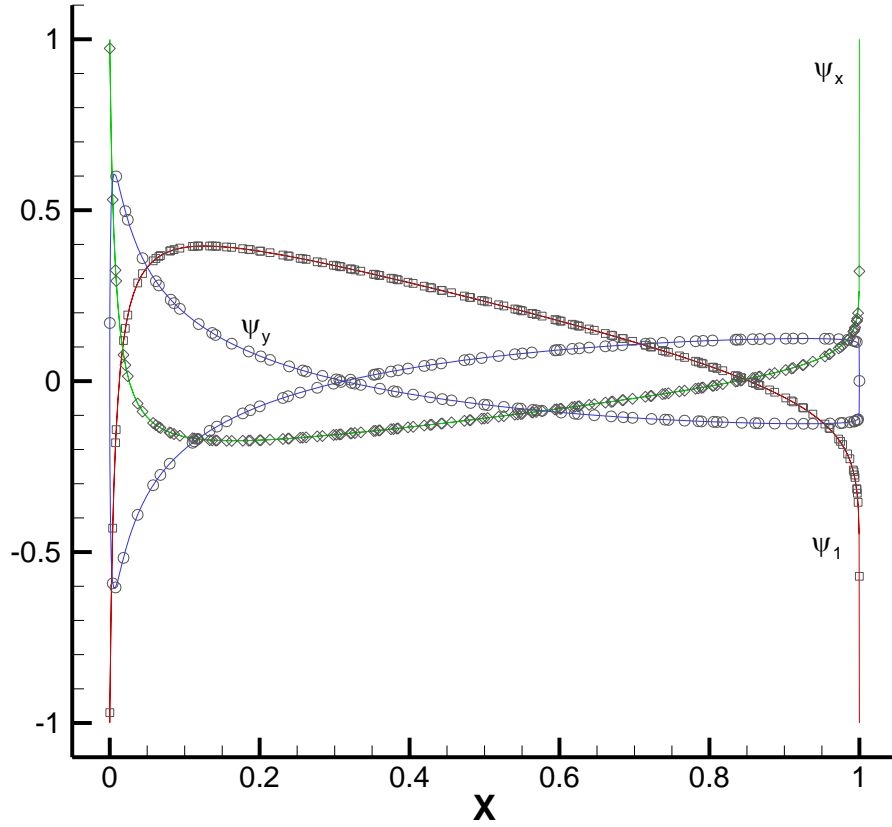


Figure 3. Analytic (solid lines) vs. numerical (symbols) drag-based adjoint solution on the airfoil profile for incompressible, inviscid flow at $\alpha = 0^\circ$ past a van de Vooren airfoil with trailing-edge angle $\tau = 16^\circ$ and 12% thickness. The numerical solution has been computed with the SU2 solver on the finest mesh of Figure 2.

As for lift, the solution is (not unexpectedly) considerably more complex,

$$\begin{pmatrix} \psi_1 \\ \psi_x \\ \psi_y \end{pmatrix}_{Lift} = \frac{q_\infty}{c_\infty} \begin{pmatrix} 2\Upsilon^{(1)} - q^2 \Xi \\ -q_\infty^{-1} \sin \alpha + u \Xi - \frac{u}{q^2} \Upsilon^{(1)} + \frac{v}{q^2} (1 + \Upsilon^{(2)}) \\ q_\infty^{-1} \cos \alpha + v \Xi - \frac{v}{q^2} \Upsilon^{(1)} - \frac{u}{q^2} (1 + \Upsilon^{(2)}) \end{pmatrix} \quad (2)$$

where the functions

$$\begin{aligned} \Upsilon^{(1)}(z) &= -i \left(\frac{\zeta_{te} - \zeta_0}{\zeta(z) - \zeta_{te}} - \frac{\overline{\zeta_{te} - \zeta_0}}{\overline{\zeta(z) - \zeta_{te}}} \right) = \\ &= 2 \frac{X_{te}(Y_0 - Y) + X_0(Y - Y_{te}) + X(Y_{te} - Y_0)}{(X - X_{te})^2 + (Y - Y_{te})^2} \\ \Upsilon^{(2)}(z) &= \frac{\zeta_{te} - \zeta_0}{\zeta(z) - \zeta_{te}} + \frac{\overline{\zeta_{te} - \zeta_0}}{\overline{\zeta(z) - \zeta_{te}}} = \\ &= 2 \frac{(X - X_0)(X - X_{te}) + (Y - Y_0)(Y - Y_{te}) - (X - X_{te})^2 - (Y - Y_{te})^2}{(X - X_{te})^2 + (Y - Y_{te})^2} \end{aligned}$$

(with $\bar{\zeta}$ the complex conjugate of $\zeta = X + iY$) describe the perturbations to the Kutta condition due to the point source and vortex, respectively (see [7] for further details), and

$$\Xi(z) = -\int_0^\infty ds \partial_s q^{-2}(\vec{x}(s)) \Upsilon^{(1)}(\vec{x}(s)) + 2 \int_0^\infty ds q^{-2} \partial_s \phi(\vec{x}(s)) (1 + \Upsilon^{(2)}(\vec{x}(s)))$$

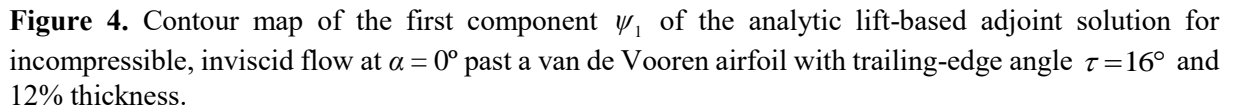
is an integral along the streamline passing through z (which corresponds to the lower limit $s = 0$, where s is the streamline coordinate measuring distance along streamlines). Here ϕ is the local flow angle. This integral comes from the stagnation pressure point perturbation and, as in [5], it is responsible for the adjoint singularity along the incoming stagnation streamline and, crucially, along the wall, as we shall see shortly.

Both $\Upsilon^{(1)}$ and $\Upsilon^{(2)}$ are singular at the trailing edge, but $\Upsilon^{(2)}$ is actually constant ($\Upsilon^{(2)} = -1$) throughout the airfoil defined by $\zeta = \zeta_0 + Re^{i\theta}$, $0 \leq \theta < 2\pi$. This behavior is crucial to preserve the adjoint wall boundary condition. In fact, it can be seen that this solution obeys the adjoint wall b.c. and the adjoint equations. The solution has a primary singularity at the trailing edge caused by $\Upsilon^{(1)}$ and $\Upsilon^{(2)}$ and, thus, by the Kutta condition, which is transported throughout the

domain by the streamline integral Ξ , which diverges along the wall. The singularities, however, remain close to the dividing streamline upstream of the trailing edge. As points get close to either the incoming stagnation streamline or the wall, the corresponding streamline approaches the singularity at the trailing edge and Ξ diverges due to the divergence at the trailing edge. The integral also gets a small contribution from the leading edge region, but it can be seen to be roughly constant upstream of the trailing edge region, and negligible downstream. The trailing edge divergence thus explains both the singularities at the incoming stagnation streamline and the wall, which in fact show identical behavior with the distance d to the streamline or the wall, $\Xi \sim 1/d^{1/2+\tau/\pi}$ [7], which is not universal since it depends on the trailing edge angle τ , and reduces to the inverse square-root behavior predicted in [5] for cusped trailing edges. Downstream of the trailing edge, though, the dividing streamline is not singular (it behaves as $\Xi \sim d$, where d is the distance to the dividing streamline) except at the trailing edge itself, where $\Xi \sim 1/d^{\frac{1+2\tau/\pi}{2-\tau/\pi}}$ and d is now the minimum distance to the trailing edge along the streamline.

Setting $\tau = \pi$ correctly reproduces the results for blunt bodies such as the circle. This may come as a surprise, since while adjoint solutions past blunt bodies do show the anomalous behavior in numerical computations, no Kutta condition is involved (a priori). However, as explained in [7], to obtain a meaningful adjoint for these cases it is necessary to impose a Kutta condition demanding that the point perturbations do not change the location of the rear stagnation point. As a consequence of this, the solution (2) also applies to those cases.

In order to examine these results in a concrete case, the analytic adjoint solution for the van der Vooren airfoil discussed earlier has been obtained by direct evaluation of (2). An important ingredient in the computation is the streamline integration, which requires prior determination of the streamline passing for a given point. This is done by direct numerical integration of the equation $d\vec{x}/dt = \vec{v}(\vec{x})$ with a fourth-order Runge-Kutta method (see e.g. [19]). The streamline tracing is performed in the circle plane and then translated into the airfoil plane via the conformal transformation (Eq. (1) in the present example). The analytic lift adjoint solution obtained in this way is shown in Figure 4.



10

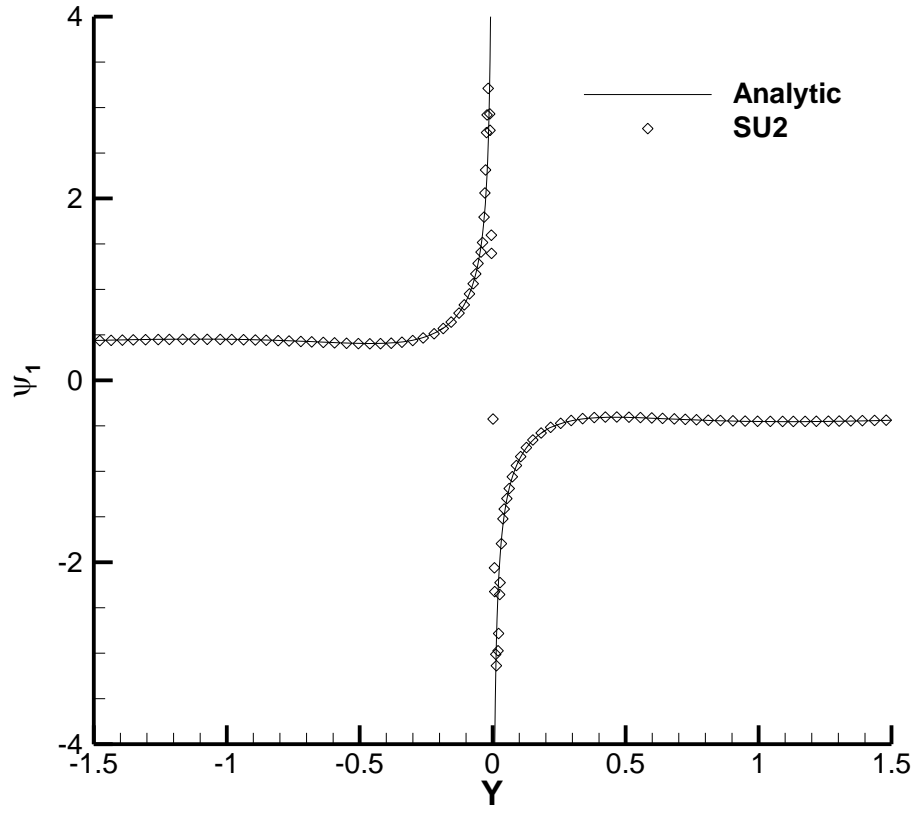


Figure 5. Plot of ψ_1 along a line crossing the stagnation streamline upstream of the airfoil as indicated in Figure 4 for incompressible, inviscid flow at $\alpha = 0^\circ$ past a van de Vooren airfoil with trailing-edge angle $\tau = 16^\circ$ and 12% thickness.

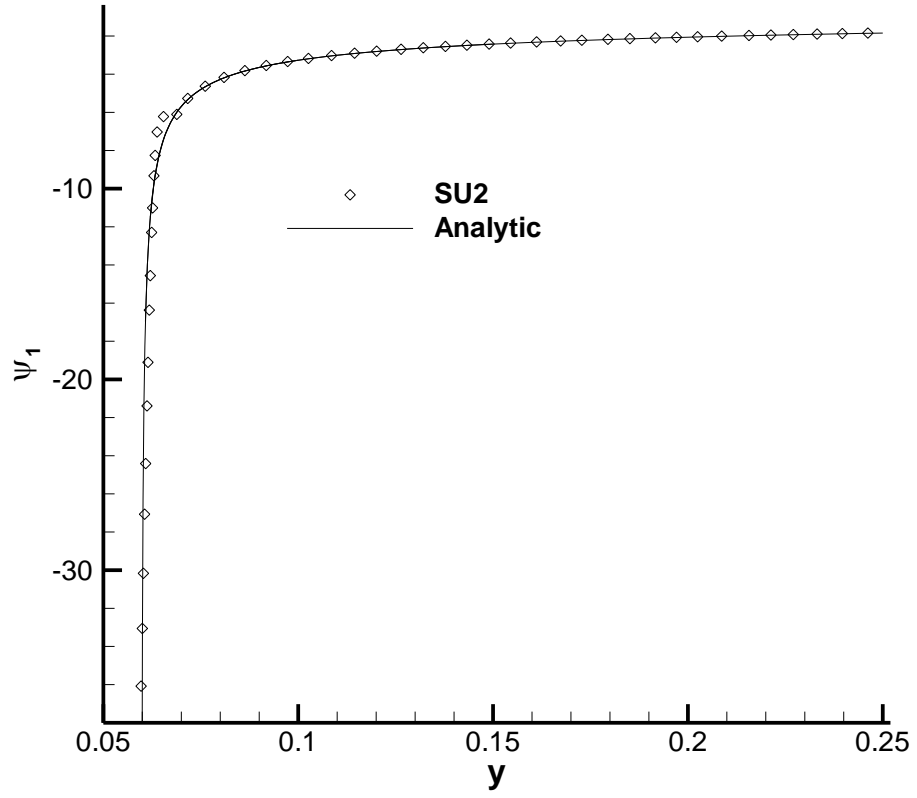


Figure 6. Plot of ψ_1 along a line normal to the airfoil wall at $x/c = 0.31$ as indicated in Figure 4 for incompressible, inviscid flow at $\alpha = 0^\circ$ past a van de Vooren airfoil with trailing-edge angle $\tau = 16^\circ$ and 12% thickness. Wall is at $y = 0.06$.

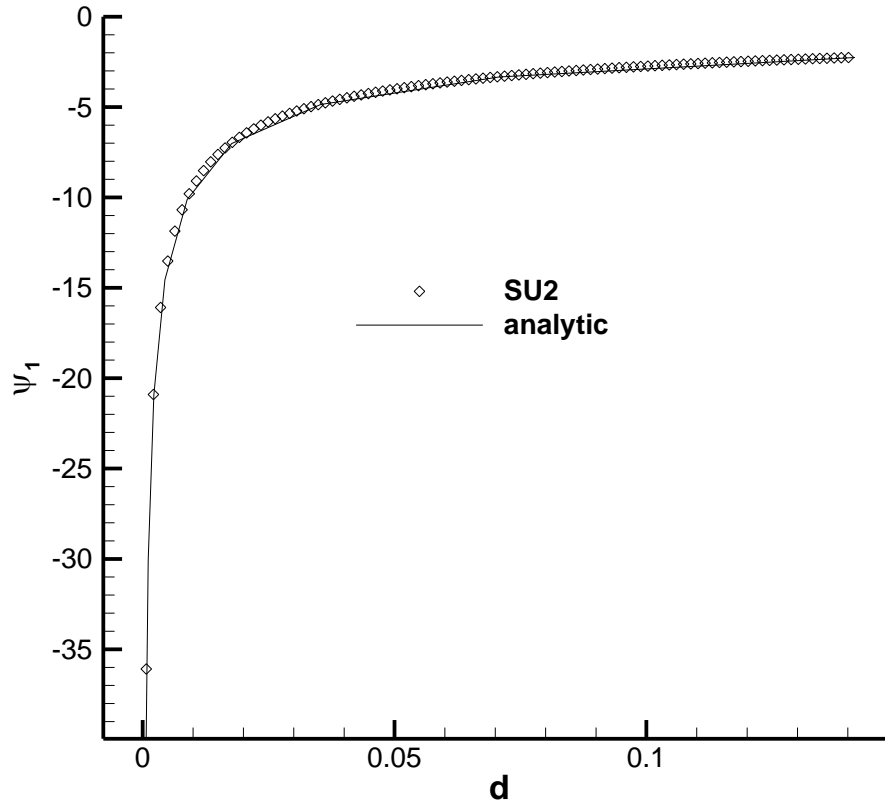


Figure 7. Plot of ψ_1 along the line $(x, y) = (1 + d / \sqrt{2}, d / \sqrt{2})$ approaching the trailing edge as indicated in Figure 4 for incompressible, inviscid flow at $\alpha = 0^\circ$ past a van de Vooren airfoil with trailing-edge angle $\tau = 16^\circ$ and 12% thickness. d denotes the distance to the trailing edge.

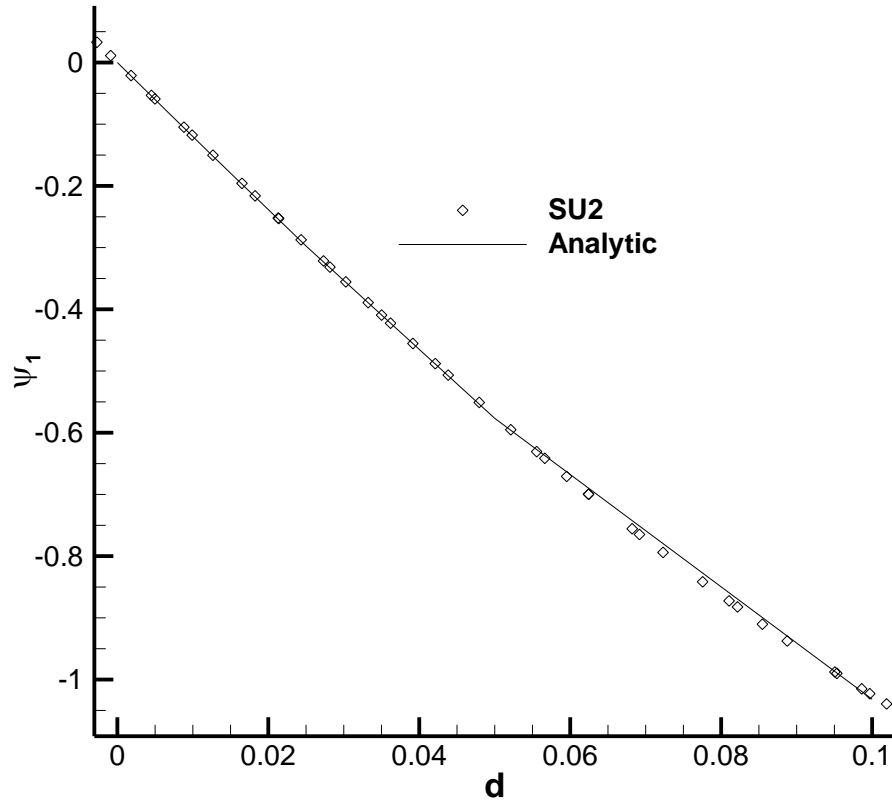


Figure 8. Plot of ψ_1 along a line crossing the stagnation streamline downstream of the airfoil as indicated in Figure 4 for incompressible, inviscid flow at $\alpha = 0^\circ$ past a van de Vooren airfoil with trailing-edge angle $\tau = 16^\circ$ and 12% thickness. d denotes the distance to the stagnation streamline.

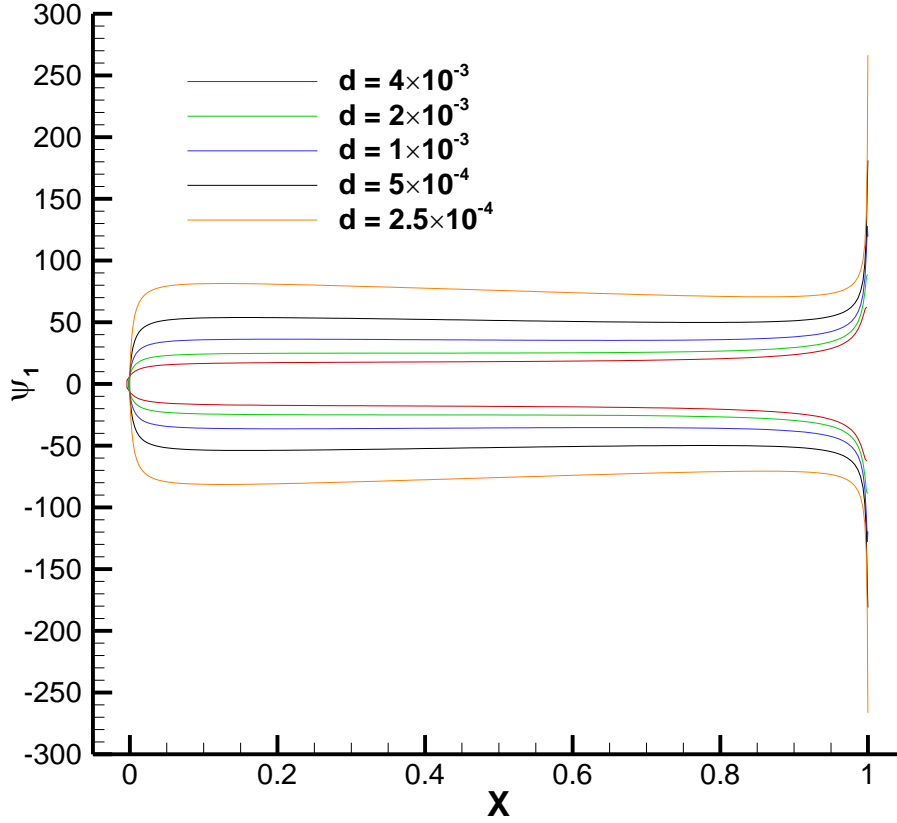


Figure 9. Analytic lift-based adjoint solution for incompressible, inviscid flow at $\alpha = 0^\circ$ past a van de Vooren airfoil with trailing-edge angle $\tau = 16^\circ$ and 12% thickness on a sequence of O-shaped curves progressively converging on the airfoil.

The behavior of the above solution is quite surprising. As was already conjectured in [4], ψ_1, ψ_x, ψ_y diverge towards the wall while the quantities

$$I^{(1)} = \psi_1 + \vec{v} \cdot (\psi_x, \psi_y) = (q_\infty \Upsilon^{(1)} - u \sin \alpha + v \cos \alpha) / c_\infty$$

$$I^{(2)} = v\psi_x - u\psi_y = (-v \sin \alpha - u \cos \alpha + q_\infty (1 + \Upsilon^{(2)})) / c_\infty$$

which yield the linearized perturbation to the lift caused by a point source and a point vortex perturbation, respectively [5] [7], remain finite except at the trailing edge. This fact is relevant since $I^{(1)}$ is related to the (continuous) adjoint-based lift/drag gradient [9]

$$\delta \int_S C_p (\vec{n}_S \cdot \vec{d}) ds = \int_{\delta S} C_p (\vec{n}_S \cdot \vec{d}) ds - \int_S (\vec{n}_S \cdot \delta \vec{v}) \rho (\psi_1 + \vec{v} \cdot (\psi_x, \psi_y)) ds \quad (3)$$

(S denotes the wall surface, $\delta \vec{v}$ is the perturbed velocity, and the first term on the right-hand side stands for the geometric variation of the objective function), while $I^{(2)}$ approaches $q \vec{n}_S \cdot (\psi_x, \psi_y)$ as the point approaches the wall and is thus directly related to the adjoint b.c. The

analytic solution for $I^{(1)}$ and $I^{(2)}$ is compared in Figure 10 and Figure 11 with the numerical adjoint solution obtained with SU2 on the sequence of meshes of Figure 2. Observe that the numerical solutions are stable against mesh refinement and agree fairly well with the analytic solution, which can thus be used for verification of numerical adjoint solvers.

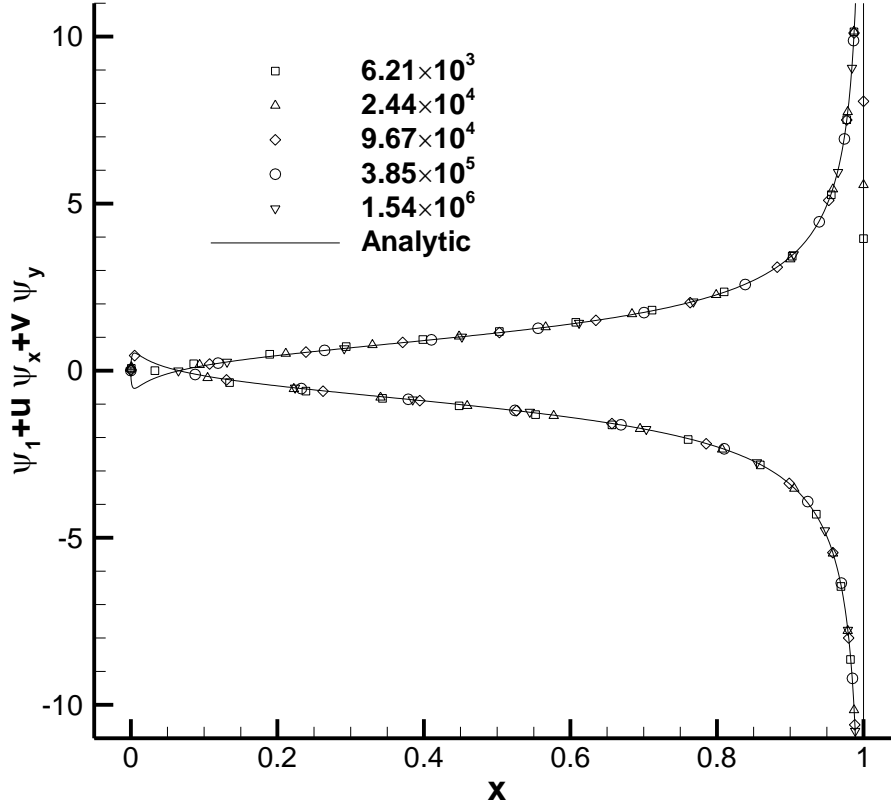


Figure 10. $I^{(1)} = \psi_1 + \vec{v} \cdot (\psi_x, \psi_y)$ computed with numerical and analytic lift-based adjoint solutions for incompressible, inviscid flow at $\alpha = 0^\circ$ past a van de Vooren airfoil with trailing-edge angle $\tau = 16^\circ$ and 12% thickness.

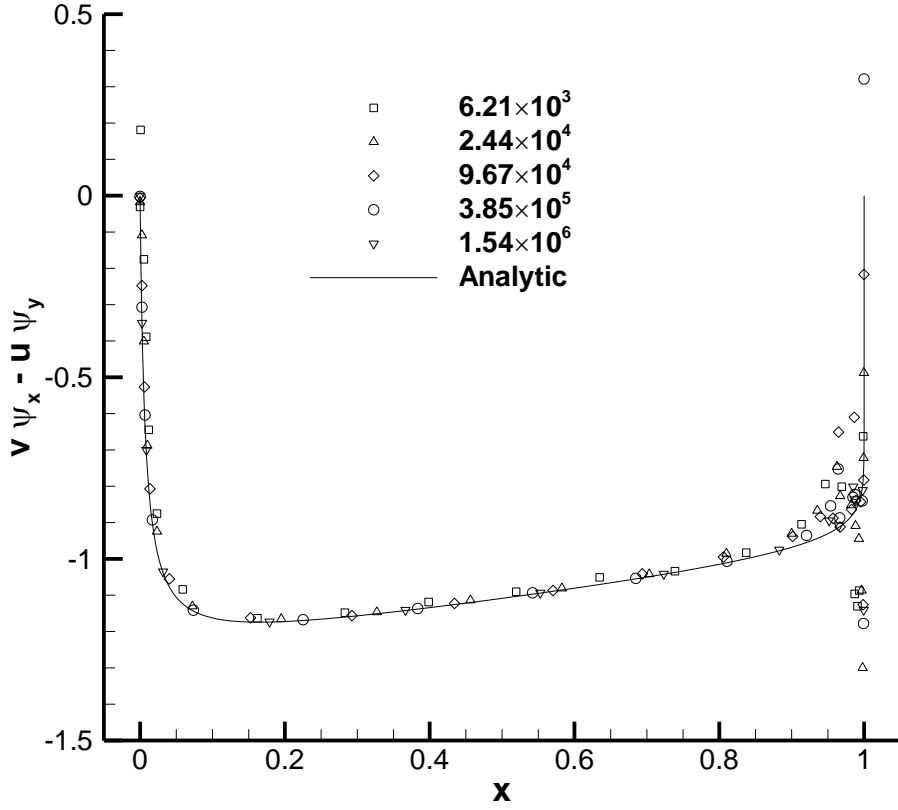


Figure 11. $I^{(2)} = v\psi_x - u\psi_y$ computed with numerical and analytic lift-based adjoint solutions for incompressible, inviscid flow at $\alpha = 0^\circ$ past a van de Vooren airfoil with trailing-edge angle $\tau = 16^\circ$ and 12% thickness.

4 SUMMARY AND DISCUSSION

Direct analysis of the behavior of the analytic lift-based adjoint solution for the incompressible Euler equations in 2D has shown that the adjoint solution is singular at the wall and the incoming stagnation streamline. The ultimate origin of both singularities is to be found in the adjoint singularity at the trailing edge, which itself is due to the sensitivity of the Kutta condition to perturbations of the flow [7] [20]. The effect of this singularity is local for point source and vortex perturbations, but extends upstream along streamlines for stagnation pressure perturbations, more increasingly so as the wall and incoming stagnation streamlines are approached, which explains the results in [5] and [6].

Numerical solutions computed with cell-vertex schemes, which place computational nodes directly on the geometry, do not show the divergence owing to numerical dissipation. The price to be paid is that now the numerical solution at the wall depends continually on the level of dissipation or the mesh density. Decreasing the dissipation or refining the mesh, which has a similar effect on the solution, changes the value of the adjoint solution at the wall. A similar

effect can be found in solutions computed with cell-centered schemes, only that now the continuous variation with mesh density affects the values computed at the near-wall cells.

The present analysis is of course restricted to incompressible flow, but we think that it is safe to extend the conclusions to compressible flows as well, at least qualitatively. Adjoint singularities at the wall, the trailing edge and the incoming stagnation streamline, which are also present for compressible flows, simply reflect the sensitivity of the lift or drag to perturbations to the Kutta condition. When such perturbations are suppressed by the flow conditions (high transonic, supersonic or viscous cases) the singularities disappear. In principle, the Kutta condition affects circulation and thus lift, with one exception: rotational transonic flow, where the Kutta condition is tied to the flow structure (the shock on the suction side and the slip line emanating from the trailing edge) [21], and any perturbation causes the displacement of the shock, resulting in drag.

The comparison between analytic and numerical results is quite impressive, even for singular solutions. Hence, the results presented here can also be used for verification of adjoint solvers. It would be nice to replicate these results for compressible flows, but the task may well be out of reach.

ACKNOWLEDGEMENTS

The research described in this paper has been supported by INTA and the Ministry of Defence of Spain under the grant Termofluidodinámica (IGB99001). The numerical computations reported in the paper have been carried out with the SU2 code, an open source platform developed and maintained by the SU2 Foundation.

REFERENCES

- [1] C. Lozano, "Watch Your Adjoints! Lack of Mesh Convergence in Inviscid Adjoint Solutions," *AIAA J.*, vol. 57, no. 9, pp. 3991-4006, 2019. <https://doi.org/10.2514/1.J057259>.
- [2] C. Lozano, "Anomalous Mesh Dependence of Adjoint Solutions near Walls in Inviscid Flows Past Configurations with Sharp Trailing Edges," in *Proceedings EUCASS 2019, Paper 291*. DOI: 10.13009/EUCASS2019-291, Madrid, 2019.
- [3] C. Lozano and J. Ponsin, "Mesh-Diverging Inviscid Adjoint Solutions," in *10th EASN International Virtual Conference, IOP Conf. Ser.: Mater. Sci. Eng. 1024 (2021) 012042*. doi: 10.1088/1757-899X/1024/1/012042, 2021.
- [4] C. Lozano and J. Ponsin, "On the Mesh Divergence of Inviscid Adjoint Solutions," in *Proceedings of WCCM-ECCOMAS2020. F. Chinesta, R. Abgrall, O. Allix and M. Kaliske, (Eds). Scipedia, Volume 1300 - Inverse Problems, Optimization and Design*. URL: https://www.scipedia.com/public/Lozano_Ponsin_2021a. DOI: 10.23967/wccm-eccomas.2020.258, 2021.

- [5] M. B. Giles and N. A. Pierce, "Adjoint Equations in CFD: Duality, Boundary Conditions and Solution Behavior," AIAA Paper 97-1850, 1997. doi: 10.2514/6.1997-1850.
- [6] J. Peter, F. Renac and C. Labbé, "Analysis of finite-volume discrete adjoint fields for two-dimensional compressible Euler flows," *preprint, arXiv:2009.07096 [physics.comp-ph]*, 2020.
- [7] C. Lozano and J. Ponsin, "Analytic Adjoint Solutions for the 2D Incompressible Euler Equations Using the Green's Function Approach," 2021 (in preparation).
- [8] J. Katz and A. Plotkin, *Low Speed Aerodynamics*, 2nd edition, New York: Cambridge University Press, 2001.
- [9] C. Castro, C. Lozano, F. Palacios and E. Zuazua, "Systematic Continuous Adjoint Approach to Viscous Aerodynamic Design on Unstructured Grids," *AIAA J.*, vol. 45, no. 9, pp. 2125-2139, 2007. doi: 10.2514/1.24859.
- [10] M. Giles and N. Pierce, "Improved Lift and Drag Estimates Using Adjoint Euler Equations," AIAA paper 99-3293. doi: 10.2514/6.1999-3293.
- [11] T. D. Economou, F. Palacios, S. R. Copeland, T. W. Lukaczyk and J. J. Alonso, "SU2: An Open-Source Suite for Multiphysics Simulation and Design," *AIAA Journal*, vol. 54, no. 3, pp. 828-846, 2016. doi: 10.2514/1.J053813.
- [12] C. Lozano, "On Mesh Sensitivities and Boundary Formulas for Discrete Adjoint-based Gradients in Inviscid Aerodynamic Shape Optimization," *J. Comput. Phys.*, vol. 346, pp. 403-436, 2017. doi: 10.1016/j.jcp.2017.06.025.
- [13] C. Lozano, "Entropy and Adjoint Methods," *J Sci Comput*, vol. 81, pp. 2447-2483, 2019. <https://doi.org/10.1007/s10915-019-01092-0>.
- [14] D. Schwamborn, T. Gerhold and R. Heinrich, "The DLR TAU-Code: Recent Applications in Research and Industry," in *ECCOMAS CFD 2006, European Conference on CFD*, Egmond aan Zee, The Netherlands, 2006.
- [15] A. Jameson, W. Schmidt and E. Turkel, "Numerical Solutions of the Euler Equations by Finite Volume Methods Using Runge-Kutta Time-Stepping Schemes," AIAA Paper 81-1259, 1981. doi: 10.2514/6.1981-1259.
- [16] D. Ekelschot, "Mesh adaptation strategies for compressible flows using a high-order spectral/hp element discretisation," Ph.D. Thesis, Department of Aeronautics, Imperial College (London), 2016.
- [17] M. B. Giles and N. A. Pierce, "Analytic adjoint solutions for the quasi-one-dimensional Euler equations," *J. Fluid Mechanics*, vol. 426, pp. 327-345, 2001. doi: 10.1017/S0022112000002366.
- [18] C. Lozano and J. Ponsin, "An exact inviscid drag-adjoint solution for subcritical flows," *AIAA Journal*, 2021 (in press).
- [19] M. Giles and R. Haimes, "Advanced Interactive Visualization for CFD," *Computing Systems in Engineering*, vol. 1, no. 1, pp. 51-62, 1990.
- [20] M. B. Giles and N. A. Pierce, "Adjoint error correction for integral outputs," in *Error Estimation and Solution Adaptive Discretization in Computational Fluid Dynamics (Lecture Notes in Computer Science and Engineering, vol. 25)*, T. Barth and H.

Deconinck, Eds., Berlin, Springer Verlag, 2002, pp. 47-95. Doi: 10.1007/978-3-662-05189-4_2.

- [21] W. Schmidt, A. Jameson and D. Whitfield, "Finite Volume Solution of the Euler Equations of Transonic Flow over Airfoils and Wings Including Viscous Effects," *J. Aircraft*, vol. 20, pp. 127-133, 1983.